Trajectory Simulations of C_{58}^+ from C_{60} in the VMI Spectrometer

B. P. Kafle[1], Md. S. I. Prodhan[1], H. Katayanagi[1, 2] and K. Mitsuke[1, 2]

[1]*Dept. Photo-Molec. Sci., Inst. Molec. Sci., Okazaki 444-8585, Japan*
[2]*Graduate Univ. Adv. Studies (SOKENDAI), Okazaki 444-8585, Japan*

The performance of the mass-selective velocity map imaging (VMI) spectrometer has been studied by the computer simulation of the ion trajectories, by taking an example of C_{58}^+ from C_{60}.

The geometry of the VMI spectrometer is given in [1] and is essentially the same as that in [2]. The lens system contains three square electrodes, *viz.* repeller, ion extractor and tube entrance, all of which have the sides of 50 mm and the internal diameters of 20 mm. The central holes of the latter two electrodes have no mesh. Such open-hole structures have enabled us to bend the equipotential surfaces simply by manipulating the ion-extractor voltage and to achieve the excellent focusing of the PSD image.

We performed ion trajectory simulations utilizing the SIMION 3D software [3] to optimize the dimensions of the electrodes. Here, dissociative ionization of C_{60} was considered to take place within a region of rectangular parallelepiped $\Delta x \Delta y \Delta z = 1 \times 3 \times 1$ mm^3. The *y*-direction was assigned to the passage of SR, so that it ranges from -1.5 to +1.5 mm. The eight corners and center of the ionization region were chosen for the starting points of the ion flights. From each point 171 trajectories were generated in the range of the elevation angle θ from $-90°$ to $+90°$ at intervals of 22.5° and in the range of the azimuth angle ϕ from 0° to $+180°$ at intervals of 10° (see [2]).

Application of the pulse voltages to the repeller and mass gate (V_R and V_G, respectively) has been realized by means of a "user program" of SIMION [3]. The base line values of all the pulse voltages were 0 V. The amplitude and duration of V_R were 300 V and 7 μs, respectively. At the same time a pulse voltage with the amplitude of 214 V was applied to the ion extractor. Such applications permit the ions produced during the past 13 μs to be guided into the drift tube. To filter C_{58}^+ ions we set the timing of V_G at 44.5 μs later than that of V_R. At the mass gate the spread of the TOF of C_{58}^+ was estimated to be 0.65 μs which arises from the finite volume of the ionization region and distribution of the kinetic energy of the fragment ions. Thus, the amplitude and duration of V_G were set to 120 V and 1 μs, respectively. A continuous voltage of 320 V was applied to the retarding grid of the ion reflector.

Most of the simulated trajectories of C_{58}^+ were found to go beyond the retarding grid and reach the PSD, whereas the trajectories of C_{60}^+ and C_{56}^+ were reflected completely. This observation may provide evidence for exclusive imaging detection of C_{58}^+ without interference from the neighboring ions, C_{60}^+ and C_{56}^+, with the same kinetic energies.

Figure 1 shows the simulated velocity map images of C_{58}^+ ions on the PSD at the kinetic energies of 0.1 eV (○) and 0.11 eV (■). It should be noted that these images result from momentum distributions of the ions in the laboratory system. We took into account the ion trajectories generated in the elevation and azimuth angle ranges of 0° to +90° and 0° to +180°, respectively, which cover only one quarter of the full 3D trajectories over the 4π solid angle. The trajectories with a given elevation angle form a horizontal stripe, and the envelope of all the stripes makes an arc, which clearly demonstrates that scattering distribution in spherical symmetry can be successfully projected on an image plane. It is likely that C_{58}^+ fragment ions with kinetic energy difference of 0.01eV are almost separable. Comparison between the simulations with and without the mass gate and ion reflector confirmed that the images are not distorted in the presence of these devices.
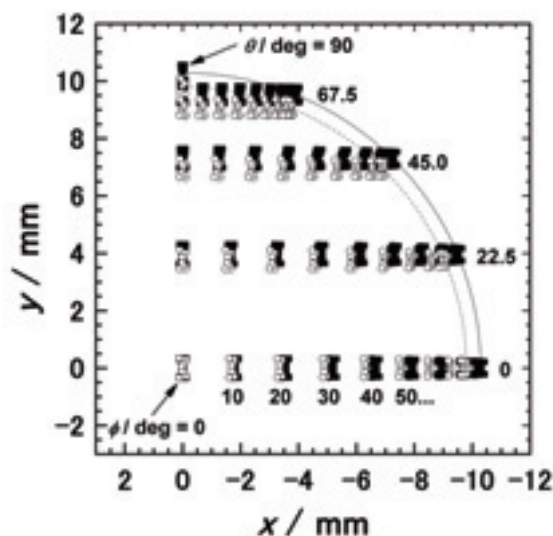
Fig. 1. Simulated 2D images of the 3D velocity distribution of C_{58}^+ from C_{60} projected on the PSD. The initial kinetic energies of C_{58}^+ were set to 0.1 (○) and 0.11 eV (■).

[1] H. Katayanagi, B. P. Kafle, C. Huang, Md. S. I. Prodhan, H. Yagi and K. Mitsuke, in the Proceed. of Pure and Applied Chemistry International Conference 2010 (PACCON2010), Thailand, PTC-PO-45.
[2] B. P. Kafle, H. Katayanagi, K. Mitsuke, AIP Conf. Proc. **879** (2007) 1809.
[3] D. A. Dahl, SIMION 3D ver. 7.0, Boise Idaho, Scientific Instrument Services Inc., 2000.

Ⅲ-2. INSTRUMENTAL DEVELOPMENTS

Performance of a High-Precision Transmission Grating with 5555-lines/mm Groove Density for High-Resolution Soft X-Ray Emission Spectroscopy

H. Yamane[1], T. Hatsui[2] and N. Kosugi[1]

[1] Institute for Molecular Science, Okazaki 444-8585, Japan
[2]XFEL Project Head Office, RIKEN & JST-PREST, Hyogo 679-5148, Japan

The X-ray emission spectroscopy (XES) measures X-rays emitted as a photon-in/photon-out process of the inner-shell excitation. The XES technique combined with the synchrotron radiation is a powerful method to investigate element-specific excitations and occupied partial density of states of gases, liquids, and solids under various conditions. However, a serious problem in the conventional XES using a grazing-incidence spectrometer based on the Rowland circle mount is a rather low quantum efficiency, arising from various factors, *e.g.*, (i) the low emission probability of ~0.1 % at the emission point, (ii) the number of focusing elements for emitted X-rays (horizontal direction only), and (iii) the low acceptance angle and low quantum efficiency at charge-coupling devices (CCD) detector with the grazing-incidence geometry in the soft X-ray region. Moreover, these factors significantly sacrifice the energy resolution. Such problems are in general solved by the use of high brilliant X-ray beam of over 10^{12}–10^{13} photons/s. In this case, however, one has to take care of radiation damage, in particular for soft materials such as organic and biomolecular systems.

In order to overcome the above problems, recently, we have developed a new type of soft X-ray emission spectrometer using a transmission grating (TG) at BL3U of the UVSOR facility [1]. The spectrometer adopts a novel optical design with a Wolter type I premirror, a free-standing TG, and a back-illuminated CCD, which enables high efficiency (~ 1 spectrum/h at 10^{11} photons/s) and high energy resolution. A self-standing TG made of silicon carbide (SiC) with the groove density of 6250 lines/mm (160 nm periods) has been evaluated as a prototype TG by NTT-AT N. However, as confirmed from the scanning electron microscopy (SEM) image, shown in Fig. 1(a), there is a distortion of the slit structure due to the resolution limit in the present electron-beam lithography method during the fabrication of TG.

In FY2009, the new TG, which is focused on the stability and accuracy of the slit structure as shown in Fig. 1(b), has been fabricated. In the new TG, the SiC thickness is about 500 nm, the groove density is 5555 lines/mm (180 nm periods), and the size of the slit is 108 nm at the surface side and 64 nm at the backside as shown in Fig. 1(c). The flatness of the TG surface is identically deflected as confirmed by a ZYGO method (not shown).

Figure 2 shows a test XES spectrum for a Si(111) wafer, measured at an incident photon energy hv_{in} = 100 eV with ΔE_{in} = 28.5 meV. We have preliminary observed a very sharp elastic peak in the Si Lα resonant XES spectrum with the full-width at half-maximum of about ΔE_{out} = 35 meV, *i.e.*, $E/\Delta E_{out}$ ~ 3000, although the alignment of the new TG optics has not yet completed as suggested by the tail structure in the elastic peak, which should be fixed by the further alignment.
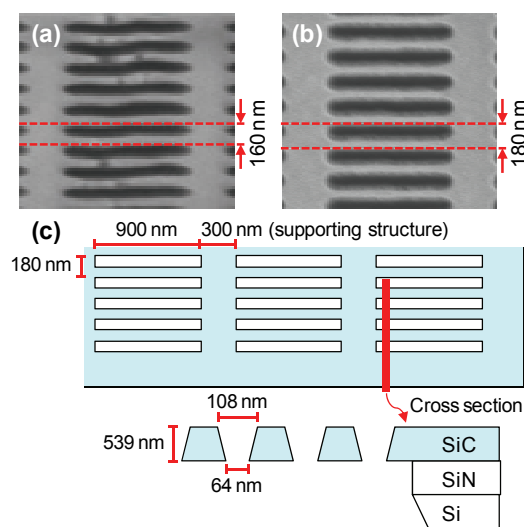
Fig. 1. SEM image for the prototype TG (a) and new TG (b) with the groove density of 6250 lines/mm (160 nm period) and 5555 lines/mm (180 nm period), respectively. (c) Basic structure of the new TG.
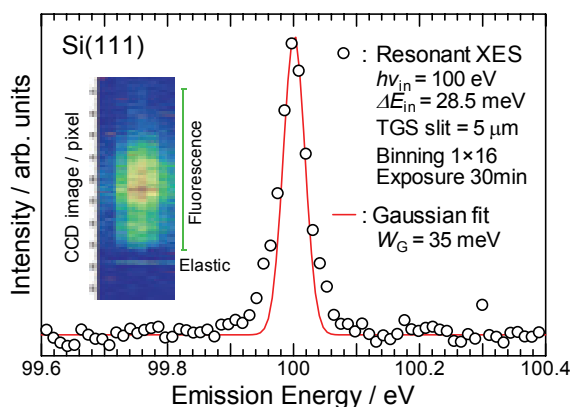
Fig. 2. Si Lα resonant XES spectrum (hv_{in} = 100 eV) for the Si(111) wafer obtained by using new TG with the best fit curve using the Gaussian function with the linewidth of 35 meV.

[1] T. Hatsui *et al.*, J. Electron Spectrosc. Relat. Phenom. **144-147** (2005) 1059.

Quantum Detection Efficiency of CsI-Coated Microchannel Plates Measured by Using Pure-Calibrated EUV Beam

G. Murakami, G. Ogawa, K. Yoshioka, H. Watanabe and I. Yoshikawa

Department of Earth and Planetary Science, Graduate School of Science,
The University of Tokyo, Tokyo 113-0033, Japan

Introduction

We study to optically observe the Earth's plasmasphere, which is filled with cold plasmas (mainly H+, He+, O+ and electrons). The He+ and O+ ions have resonance scattering emission lines in the extreme ultraviolet (EUV) region, at 30.4 nm (HeII) and 83.4 nm (OII) respectively. The intensity of each emission is proportional to column density of each scattered particle under the assumption of the optically thin condition.

Microchannel plate (MCP) detection systems have been widely used in a variety of laboratory and space applications to detect EUV radiations. EUVI (Extremity Ultra-Violet Imager) for the ISS-IMAP mission (Ionosphere, Mesosphere, upper Atmosphere and Plasmasphere mapping onboard the International Space Station) is under development. The instruments consist of band-pass filters and MCP detectors. The top MCP surface is covered with cesium iodide (CsI) photocathode in order to enhance the quantum detection efficiencies (QDEs).

It is very important to get the absolute efficiency of the instrument in order to grasp the plasma density properly. In this experiment, we measure the QDE of the MCPs which we use as a standard detector in our laboratory and evaluate the effect of CsI on the QDE.

Measurement and Result

We install an Al/Mg/Al (744Å/3958Å/747Å) filter and an Sn (1730Å) filter on the entrance of the SOR beam to eliminate the multi-order lines from 30.4nm and 58.4 nm lines, respectively. At first, we investigate the purity of each line through the entrance filter. We judge the purity from the consistency between the wavelength characteristics of an Al/Mg/Al sample filter for the continuous lines at UVSOR and those for the particular lines at the EUV facilities of Institute of Space and Astronautical Science (ISAS). The latter is measured for the emission lines of the helium gas with the discharge light source. Fig. 1 shows the transmittances of the sample filter measured at UVSOR and at ISAS. The Al/Mg/Al filter and the Sn filter are used as the entrance filter at UVSOR for 30.4 nm (Fig. 1a) and 58.4 nm (Fig. 1b), respectively. It is clear that both transmittances of the filter are consistent at 30.4 nm and 58.4 nm. We interpret from the result that the pure 30.4nm and 58.4 nm lines can be introduced through each entrance filter by using PGM35.

With the available pure lines, then we measure the QDEs of the MCP detector. The half area of the top MCP is covered with CsI and the other area is bare (without CsI). The QDEs are calculated by the rate of the MCPs count to the electron yield of the photo diode which is absolutely calibrated. Table 1 shows the result of the measurement. It shows that the QDE of CsI is higher than that of bare MCP by 1.2 at 30.4 nm and 1.5 at 58.4 nm respectively.

For the next step, in addition to the 30.4nm and 58.4 nm lines, we plan to measure the QDE at the 83.4 nm line. Then the purity of 83.4 nm line is essential, and must be investigated for the next machine time.
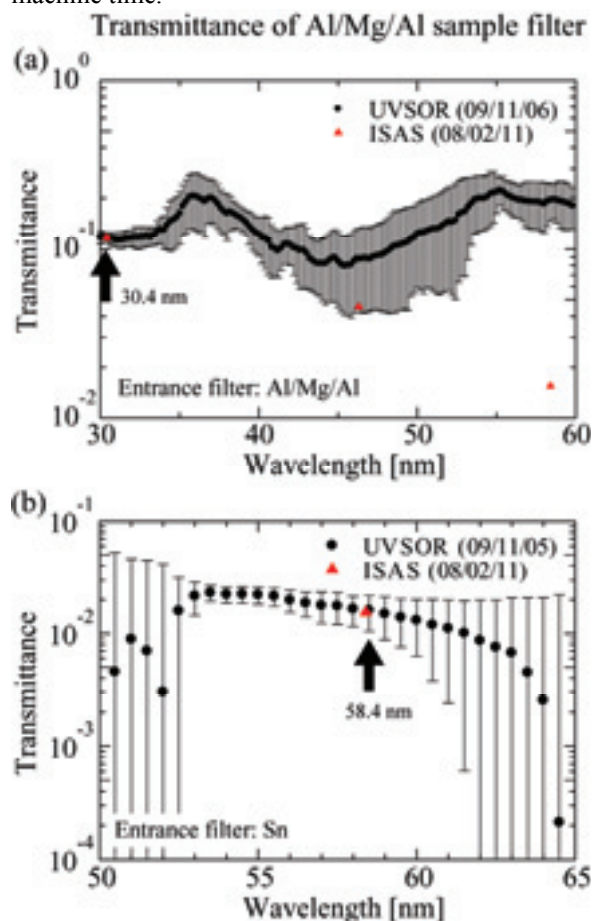
Fig. 1. The transmittances of the Al/Mg/Al sample filter measured at UVSOR and at ISAS. The Al/Mg/Al filter and the Sn filter are used as the entrance filter at UVSOR for (a) 30.4 nm and (b) 58.4 nm, respectively.

Table 1. QDEs of the MCP detector

	30.4 nm	58.4 nm
Bare	3.45±0.06%	13.04±1.71%
CsI	4.13±0.07%	19.41±2.24%

Construction of a New Experimental Setup with a High-Resolution Electron Spectrometer for Gas Phase Spectroscopy on BL6U

E. Shigemasa, E. Nakamura, N. Kondo and T. Horigome

UVSOR Facility, Institute for Molecular Science, Okazaki 444-8585, Japan

A new project for constructing the undulator beamline BL6U has been started since 2007. We have decided to choose the entrance slit-less configuration for the monochromator, as a result of the successful installation of such a configuration to BL7U. In order to cover a wide photon energy region (30-500 eV) with one single grating, a variable-included-angle Monk-Gillieson mounting has been selected. The practical construction of BL6U has begun from the summer shutdown in 2008. The first light through the monochromator has been observed in December 2008 and then precise tunings of the monochromator have been continued. It has been confirmed through its performance tests that the monochromator designed can cover the photon energy ranging from 40 to 400 eV with the resolving power higher than 5000 and the photon flux more than 10^{11} photons/sec, when the storage ring is operated in the top-up mode.

Parallel to the construction program of BL6U, the installation of a new electron spectrometer for gas phase spectroscopy has been planned. It is well known that high-resolution electron spectroscopy is a powerful tool to investigate electronic structures of atoms and molecules, especially when high-resolution electron spectra and their polarization dependences are measured as a function of photon energy in high-resolution mode. The ability of this two dimensional (2D) electron spectroscopy has been demonstrated in our recent work at SPring-8 [1], where a special attention is paid for detecting slow electrons following core excitations. In order to apply high-resolution 2D electron spectroscopy to the investigation of the L-shell excitations of the second row elements, a new experimental setup for BL6U has been designed and constructed. As a high performance hemispherical electron energy analyzer, MBS-A1, developed by the MB Scientific AB company, has been selected.

Figure 1 shows a photograph of the experimental setup, which is roughly composed of a vacuum chamber, a rotational mechanism, an MBS-A1 analyzer, a gas cell, and a double layer mu-metal screen. The analyzer is rotatable around the photon beam axis. The vacuum chamber and the rotational mechanism have been designed at UVSOR, and fabricated by TOYAMA Co., Ltd. The other components of the experimental setup have been designed by MBS, and all the components related to MBS have been transported and assembled at UVSOR in August 2009.

In order to check the performance of the analyzer, autoionizing electrons from atoms and molecules have been measured, since their peak widths are determined by the lifetimes, which are independent on the photon energy resolution. One example of the spectra obtained is given in Fig. 2, which corresponds to the autoionization peaks from Ar^+* populated by the recapture of the 2p photoelectron from Ar due to the near threshold ionization. The narrowest peak width observed is about 4 meV (FWHM) including the Doppler broadening of ~2.9 meV, which indicates the high performance of the present experimental setup. The development of software to realize 2D electron spectroscopy is in preparation.
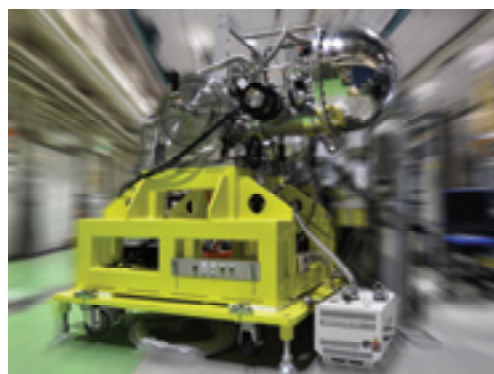
Fig. 1. Photograph of a new experimental setup for gas phase electron spectroscopy at BL6U.
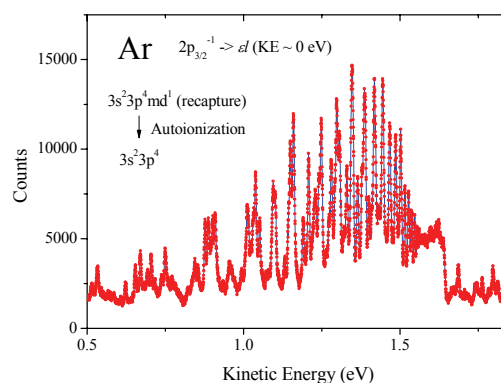
Fig. 2. Autoionization spectrum following the 2p photoionization of Ar.

[1] T. Kaneyasu, Y. Hikosaka, P. Lablanquie, F. Penent, L. Andric, G. Gamblin, J.H.D. Eland, Y. Tamenori, T. Matsushita and E. Shigemasa, Phys. Rev. Lett. **101** (2008) 183003.

Development of a High-Resolution Angle-Resolved UV/SX Photoemission Spectroscopy System for Solid Surface Study at BL6U

H. Yamane[1], T. Horigome[1], S. H. Kang[2], M. Nagasaka[1], H. W. Yeom[2] and N. Kosugi[1]

[1] *Institute for Molecular Science, Okazaki 444-8585, Japan*
[2] *CAWL, Yonsei University, Seoul 120-749, Korea*

Recently, a new undulator beamline BL6U, which covers the photon energy (hv) of 40–600 eV with the resolution power ($E/\Delta E$) of 10^4 at 10^{11}–10^{12} photons/s, has been constructed. Beside the development of a gaseous high-resolution photoemission spectroscopy system at BL6U [1], we have developed a high-resolution angle-resolved photoemission spectroscopy (ARPES) system for solid and surface study.

Our ARPES system consists of an analysis chamber, sample preparation chamber, and load-lock chamber. In the analysis chamber, we have installed a (i) high- resolution angle/spatially-resolved electron analyzer (A1ER-SES200), (ii) liquid-helium (LHe) flow cryostat (Janis ST-400 UHV) with a compact 5-axes manipulation system, and (iii) low-energy electron diffraction optics with a micro-channel plate (OCI MCP-LEED). **The MCP-LEED optics** realizes the significantly reduced sample current ($\mu A \rightarrow nA \sim pA$), and thereby, one can apply the LEED technique to soft materials such as organic thin films without the radiation damage by electrons. Thus, the combination of (i)–(iii) allows the high-precision ARPES and photoelectron diffraction (PED) experiments.

The A1ER-SES200 system (MBS A1 combined with the SCIENTA SES-200 hemispherical electron analyzer) gives a very sharp Xe $5p_{3/2}$ peak with the full-width at half-maximum of 4.6 meV at the pass energy (E_p) of 5 eV can be achieved (*cf.* 3.8 meV at $E_p = 1$ eV). In the angle-resolved mode, the electron acceptance angle (θ) is ±6–7°.

For the precise ARPES and PED experiments, we have designed and constructed **the compact LHe 5-axes manipulator** (Fig. 2). An azimuthal rotation (ϕ) is controlled by the motorized worm-&-wheel and bevel gears, which have allowance for the small backlash and the small thermal expansion between room and LHe temperature. The LHe temperature is transferred from the cryostat to samples via the copper braids. At the present diameter of the copper braids, the maximum ϕ rotation is about ±50°, and the lowest temperature at the sample position is about 20–25 K. At this low temperature, the total energy resolution (ΔE_{tot}), which includes the broadening factors from the analyzer, incident photon beam, and temperature, is obtained to 9.9 meV at $hv = 43.2$ eV and $E_p = 5$ eV for the common use, as confirmed from the ARPES spectrum for the Fermi edge of an evaporated polycrystalline Au film (Fig. 3).

The scheduled ARPES/PED experiments at BL6U are organic semiconductor films and interfaces, and adatoms (or small molecules) on metal surfaces.
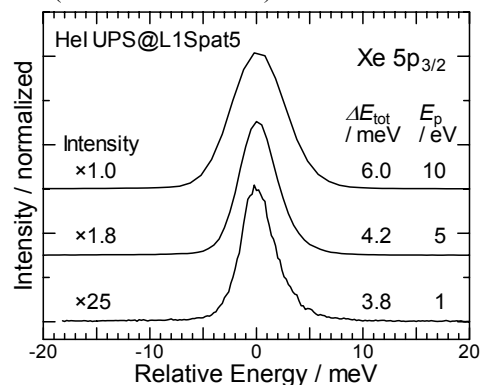
Fig. 1. Xe $5p_{3/2}$ peak obtained by using a Gammadata VUV5000 He lamp and the A1ER-SES200 system at $E_p = 1$, 5, and 10 eV.
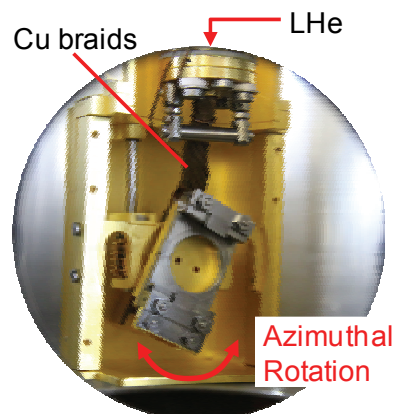
Fig. 2. Photo of the LHe 5-axes manipulator without a front radiation shield and a sample-mounting puck.
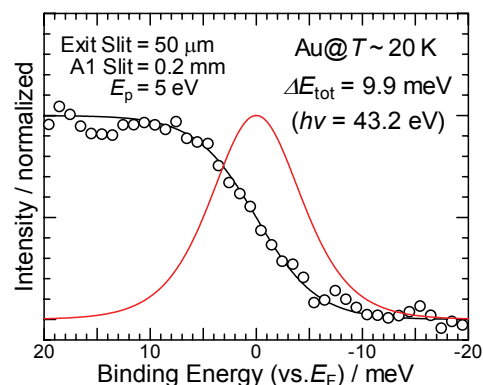
Fig. 3. Fermi edge of Au film measured at $E_p = 5$ eV, $hv = 43.2$ eV, and $T \sim 20$ K.

[1] E. Shigemasa *et al.*, UVSOR Activity Report **37** (2010) a separate page in this volume.

Ⅲ-2. INSTRUMENTAL DEVELOPMENTS

Measurement of Grating Reflectivity and Ghost Image Created by MgF$_2$ Plate

R. Ishikawa[1,2], D. Fujimura[1,3], K. Ueda[1,2], H. Watanabe[4], T. Bando[1], T. Kobiki[1],
N. Narukage[1], H. Hara[1], R. Kano[1] and S. Tsuneta[1]

[1]Hinode Science Center, National Astronomical Observatory of Japan, Mitaka 181-8588, Japan

[2] Department of Astronomy, University of Tokyo, Bunkyo-ku 113-0033, Japan

[3]Department of Earth & Planetary Science, University of Tokyo, Bunkyo-ku, 113-0033, Japan

[4]Kwasan and Hida Observatories, Kyoto University, Yamashina-ku 607-8417, Japan

We are developing instruments for Chromospheric Lyman-Alpha SpectroPolarimeter (CLASP), which will be on board NASA sounding rocket. With this rocket experiment, we will explore the magnetism of solar outer atmosphere (chromosphere and transition region) with the Hanle effect in the Ly-alpha line at 121.6 nm.

Measurement of grating reflectivity at 121.6 nm

The estimation of the grating reflectivity is critical for the development of CLASP spectrograph, since the high throughput is required to achieve the high polarization sensitivity of 0.1 – 0.3%. However, we did not have any information about the grating reflectivity at 121.6 nm. Hence we planned to actually measure the reflectivity of an existing grating by ourselves as a reference.

We borrowed the Toroidal Varied Line Space (TVLS) grating from NASA MSFC for the measurement. The groove number and the applied coating (Al/MgF$_2$) of this TVLS grating are the same as what we plan to develop. Fig. 1 shows the test setup for our measurement. We set the incident angle to 12° which is consistent with the designed one for CLASP, and measured the reflectivity at 121.6 nm for the vertical (aligned to rulings) and the horizontal (wavelength dispersion) polarization. We had already developed a beam cleaner using UV radiation at BL7B, and were able to make perfect linear polarization light in vertical and horizontal direction combined with MgF$_2$ waveplate. Though this grating is not optimized for Ly-alpha line, we found that its reflectivity was 17.5% and 14.4% in horizontal and vertical polarization, respectively, and there was no significant difference in the reflectivity between two polarizations. These values are higher than what we expected before. On the basis of the conservative estimation of CLASP throughput with these values, we confirmed that our instrument achieves the high polarization sensitivity of 0.1-0.3 %. We note that the CLASP gratings will be optimized for Ly-alpha, and we will obtain higher throughput.

Measurement of ghost image

The polarization beam splitter in CLASP is made of MgF$_2$ plate, and the reflection from its back surface creates a ghost image. This issue also should be kept in mind for the CLASP spectrograph design. Using CCD, we took images of a main beam and a ghost image produced by MgF$_2$ plate with the thickness of 0.5 mm at 121.6 nm. The CCD was located around the focus position of BL7B. It was found that the intensity ratio of the ghost to the main beam was 25%, and the difference in the positions imaged on the CCD was 2.2 mm (Fig. 2). This information will be helpful for our design of CLASP.

Finally, we briefly report the properties of the beams at BL7B with G2 grating which we noticed in our measurement. (1) The beam size became larger in vertical direction with widening slit width of G2 grating from 10 um to 500 um. (2) The 121.6 nm beam in the 1st order was imaged on our CCD, i.e., around the focus position of BL7B, 0.8 mm and 10 mm away in horizontal and vertical direction, respectively, from the 0th order beam, when the slit width was 10 um.
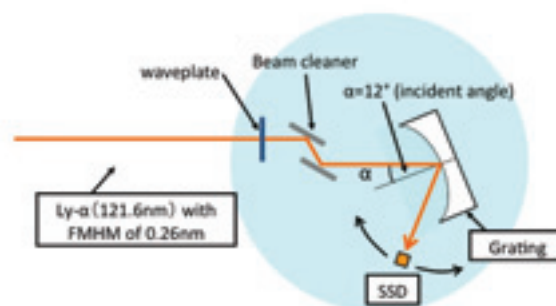
Fig 1.   Setup of grating reflectivity measurement for the vertical polarization.

Fig. 2.   Main beam and ghost image induced by MgF$_2$ plate with the thickness of 0.5 mm at 121.6 nm with the slit width of 300 um.

Development of MgF$_2$ Waveplate and Polarization Analyzer

H. Watanabe[1], N. Narukage[2], D. Fujimura[2], K. Ueda[2], R. Ishikawa[2], T. Kobiki[2] and T. Bando[2]

[1]Kwasan and Hida observatories, Kyoto University, Kyoto 607-8417, Japan
[2]National Astronomical Observatory of Japan, Mitaka 181-8588, Japan

We developed a half waveplate and a polarization analyzer made of MgF$_2$ for Lyman-alpha line (121.6 nm) by means of UV radiation at BL7B with the G2 grating. This is the basic experiment for "Chromospheric Lyman-Alpha Spectro-Polarimeter (CLASP)" rocket, which is planned to be launched in 2013. CLASP rocket will measure the weak vector magnetic field in the solar chromosphere using Lyman-alpha wavelength. As the magnetic field in the solar chromosphere is very weak, the signal is dominated by linear polarizations from the Hanle effect [1]. Our method is to measure the linear polarization by taking the spectra of two orthogonal polarization states simultaneously with a rotating half waveplate and two polarization analyzers (one of the analyzers works as a beam splitter).

MgF$_2$ is a transparent crystal for UV wavelength above 110 nm, and has birefringency with one slow axis (ne: extraordinary refractive index) and two fast axes (no: ordinary refractive index). In order to evaluate the performance of MgF$_2$ polarization analyzer, we measured the reflection/transmission (R-T) ratio as a function of the incident angle for both p-polarized (the electric vector parallel to the optical surface) and s-polarized (electric vector perpendicular to the optical surface) light. The reflected beam at Brewstar's angle is almost purely polarized consisting of s-polarized component, and thus is useful as a polarization analyzer. By fitting the R-T ratios shown in Fig. 2 , we found that the *the Brewstar's angle of MgF$_2$ is 59°*, and *121.6 nm beam at BL7B is 89% linearly polarized in the horizontal direction*. The reflection ratio at Brewstar's angle is 29.4% for s-polarized and 0.30% for p-polarized component.

As the retardation measurement needs highly linearly polarized light source, we set a beam cleaner at the entrance of the chamber. The beam cleaner is made of one Aluminum plate and one MgF$_2$ plate both located at incident angle of 60° (~Brewstar's angle for MgF$_2$), and makes perfect linear polarization light in horizontal direction (see Fig. 2).

The half waveplate for Lyman-alpha is also made of MgF$_2$ by stacking two plates whose slow axes are perpendicular to each other and whose thicknesses slightly differ from each other. The retardation of a waveplate is proportional to the product of the thickness difference and (ne-no). For developing a half waveplate, the accurate value of (ne-no) is necessary. There are few early works which measured (ne-no) [2]. We measured the retardation of three kinds of waveplates with thickness differences of 7.03 um, 8.46 um, and 14.04 um. *We deduced the value of (ne-no) is 0.0035 +/- 0.00018 at 121.6 and the thickness difference for a Lyman-alpha half waveplate is 17.18 um.* We are developing the half waveplate for Lyman-alpha line using this result. On the basis of R-T ratio and retardation measurements, we can derive the optical constants of MgF$_2$ at 121.6 nm as no=1.63, k=1.0 x 10^{-6}. We are going to submit these results to the Journal of the Optical Society of America in 2010 (the title will be "Optical Constant of MgF$_2$ Plate at Lyman-Alpha Wavelength for CLASP Experiment").
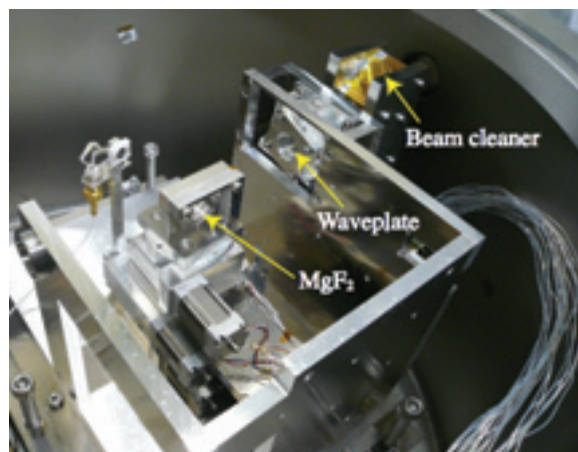
Fig. 1. Photo of our measurement system. The position of the waveplate and MgF$_2$ plate are controlled by the stepping motors.
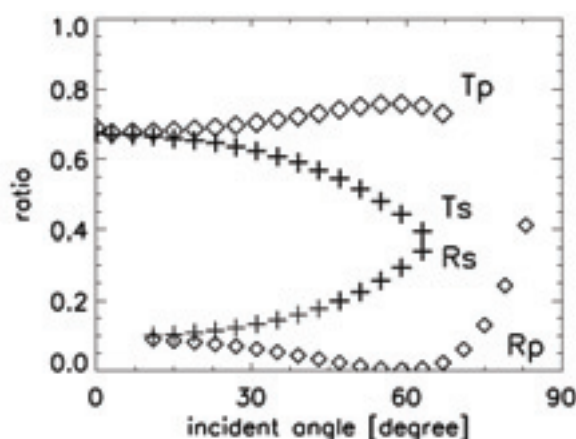
Fig. 2. Result of reflection/transmission ratio measurement.

[1] J. Trujillo Bueno and A. Asensio Ramos, Astrophysical Journal **655** (2007) 642.
[2] P. Laporte *et al*., J. Opt. Soc. Am. **8** (1983) 1477.